

# **RESTOLINK**

## **Sampling protocol**

25<sup>th</sup> of July 2025

**Clara Mendoza-Lera<sup>1</sup>, Christine Anlanger<sup>1,2</sup>, Julia Pasqualini<sup>2</sup>, Patrick Fink<sup>2,3</sup>, Isabel Muñoz<sup>4</sup>, Daniel von Schiller<sup>4</sup>, Markus Weitere<sup>2</sup>, Andreas Lorke<sup>1</sup>, Andrea Butturini<sup>4</sup>, Björn Gücker<sup>5</sup>, Davi Gasparini Fernandes Cunha<sup>6</sup>, Lidia Cañas Ramirez<sup>4</sup>, Francesc Sabater<sup>4</sup>, Ryan Sponseller<sup>7</sup>, Margarita Menendez Lopez<sup>4</sup>, Lina Polvi-Sjöberg<sup>8</sup>, Nicolás Finkler<sup>6,7</sup>, Mario Brauns<sup>2,\*</sup>**

<sup>1</sup> RPTU, Institute for Environmental Sciences (iES), Forststr. 7, 76829 Landau, Germany

<sup>2</sup> Department River Ecology, Helmholtz Centre for Environmental Research – UFZ, Brückstr. 3a, 39114 Magdeburg, Germany

<sup>3</sup> Institute of Zoology, University of Cologne, Zùlpicher Straße 47b, 50674 Köln, Germany

<sup>4</sup> Departament de Biologia Evolutiva, Ecologia i Ciències Ambientals (BEECA), Universitat de Barcelona (UB), Barcelona, Spain

<sup>5</sup> Universidade Federal de São João del-Rei (UFSJ), Campus Tancredo Neves, 36301-360 – São João del-Rei, Brazil

<sup>6</sup> São Carlos School of Engineering, University of São Paulo, Brazil

<sup>7</sup> Department of Ecology, Environment and Geoscience, Umeå University, Sweden

<sup>8</sup> Department of Forest Ecology and Management, Swedish University of Agricultural Sciences, Sweden

\*Corresponding author: [mario.brauns@ufz.de](mailto:mario.brauns@ufz.de)

# Content

1. Introduction .....	3
2. Site selection.....	4
3. Sampling design .....	5
4. General sampling procedure .....	6
5. Hydromorphology.....	8
5.1 Spot- and patch-scale hydromorphology.....	8
5.1.1 <i>Hydraulic descriptors at the spot scale</i> .....	8
5.1.2 <i>Morphological measurements at the patch scale</i> .....	10
5.2 Reach-scale hydromorphology.....	12
6. Microbial community structure and function (spot scale).....	13
6.1 Microbial community sampling .....	14
6.2 Field processing of microbial samples.....	15
6.2.1 <i>Bacteria abundance and Chlorophyll-a</i> .....	15
6.2.2 <i>Microbial diversity and stable isotope uptake</i> .....	16
6.3 Microbial community laboratory analysis and data processing .....	16
6.3.1 <i>Bacterial abundance</i> .....	16
6.3.3 <i>Microbial diversity</i> .....	16
6.3.4 <i>Biofilm <sup>13</sup>C-DOC and <sup>15</sup>N-NO<sub>3</sub><sup>-</sup> uptake</i> .....	16
7. Macroinvertebrates structure and function (patch scale).....	18
7.1 Community structure .....	18
7.2 Function .....	18
7.2.2 <i>Trophic niche width</i> .....	19
7.2.3 <i>Food web - Mixing modeling</i> .....	19
7.2.4 <i>Organic matter fluxes</i> .....	19
7.2.5 <i>Food web structure</i> .....	19
8. Ecosystem functioning (reach scale).....	20
8.1 Whole-reach DOC and N-NO <sub>3</sub> uptake.....	20
8.2 Organic matter decomposition.....	20
8.3 Whole-reach metabolism (GPP, ER, NEP) .....	20
8.3.1 <i>Gas exchange determination</i> .....	21
8.3.2 <i>Bayesian inverse model</i> .....	22
8.4 Greenhouse gas (GHG) fluxes .....	24
9. References.....	25

## 1. Introduction

The following document contains the protocols for sampling, sample processing, and data analysis of the RESTOLINK project.

Restoration measures to improve in-stream hydromorphology are increasingly adopted worldwide but often fail to recover good ecological status as well as biodiversity. Yet, the evidence for the dominant effects of hydromorphology on biodiversity and ecosystem functioning suggests that the strong potential for hydromorphological restoration is not fully explored in stream restoration. We argue that restoration often fails because it does not consider the spatial scales of stream hydromorphology that are most relevant to biodiversity and ecosystem functioning. Moreover, traditional indicators of restoration success, based on the composition of biological communities, may not reflect the same recovery trajectory as key ecosystem functions. We propose a novel framework for evaluating restoration success by mechanistically linking three central facets of stream ecosystems: hydromorphological heterogeneity at relevant scales, multi-group biodiversity (including both microbial and macroinvertebrate communities), and ecosystem multifunctionality. More specifically, in RESTOLINK, we:

- i) identify scales of hydromorphology that need to be restored to induce recovery of microbial and macrobial biodiversity (i.e. macroinvertebrates),
- ii) decipher the role of biodiversity for ecosystem functioning,
- iii) establish ecosystem functions as novel targets for freshwater restoration,
- iv) determine thresholds of biodiversity that must be restored to maximize ecosystem multifunctionality, and
- v) evaluate the uncertainties of biodiversity and functional restoration targets across biomes.

In doing so, RESTOLINK makes a significant contribution to the implementation of the European Union's Biodiversity Strategy for 2030, as well as the European Water Framework Directive. Functional indicators delivered by RESTOLINK will allow for implementation of the Aichi Biodiversity Targets, which consider biodiversity and ecosystem functioning as environmental commodities at risk.

RESTOLINK is funded by:

- UFZ and RPTU were funded by the 2020-2021 Biodiversa+ and Water JPI joint call for research projects, under the BiodivRestore ERA-NET Cofund (GA N°101003777), with the EU and the funding organizations Federal Ministry of Education and Research, Germany, grant numbers 16LW0175 and 16LW0174K.
- UB was supported by Grant PCI2022-132930 funded by MCIN/AEI/10.13039/501100011033 and by the European Union NextGenerationEU/PRTR.
- UFSJ was funded through São Paulo Research Foundation (FAPESP) – Process Number 2021/04399-1
- SLU was funded through the Swedish Environmental Protection Agency (Naturvårdsverket), grant # 2022-00035.

## 2. Site selection

RESTOLINK adopts a biome approach and evaluates restoration success in four regions (Table 1). Within each biome, we select three control-impact-restored triplets in three different streams or alternatively within the same stream segment. Streams should be permanently flowing, preferentially draining sub-mountain to mountain catchments, have 2<sup>nd</sup> to 3<sup>rd</sup> Strahler order, and have water depths >10 cm. The discharge should be <300 L/s, and NO<sub>3</sub>-N concentrations should be <2 mg/L. Candidate streams must have been subjected to hydromorphological restoration measures at least five years before sampling. We define hydromorphological restoration as a measure that will produce a quantifiable effect on stream bed characteristics and/or stream hydraulics. The type of restoration measure can differ among sites, i.e., it is possible to select three different measures within each biome to cover typical region-specific restoration measures.

**Table 1.** The four biomes and corresponding country and climate classification following Köppen-Geiger involved in RESTOLINK.

Biome	Country	Köppen-Geiger climate
Cerrado/Atlantic Rainforest	Brazil	Cwa, Aw
Temperate broadleaf forest	Germany	Cfb
Mediterranean	Spain	Cfa
Subarctic (Boreal)	Sweden	Dfc

Other major human impacts that may affect restoration success, such as agricultural land use, should be avoided. Each restored reach should be accompanied by a control and an impacted reach to form a control-restored-impact triplet. The control reach should be in a pristine catchment with native vegetation and minor human impact. The impact reach should exhibit the hydromorphological degradation present in the restored reach before the restoration measure took place. If other human stressors affecting the restored reach are inevitable, the control and impacted reach should be subjected to the same stressor.

The length of the individual restoration measure defines the reach scale in RESTOLINK. Control and impact reaches should have comparable lengths. Reaches should be sufficiently long to include the entire area affected, e.g., including impounded areas upstream of low-head dams. The three reaches that make up a triplet should be as homogeneous as possible and should lack tributaries, and have homogeneous canopy cover as well as comparable slope, width, geomorphic complexity and valley confinement.

### 3. Sampling design

RESTOLINK follows a nested sampling design at four spatial scales following the spatially nested hierarchy of fluvial habitats from microhabitat ( $\sim 10^{-2} - 10^{-1}$  m, hereafter spot for microbial community and patch for macroinvertebrates) and mesohabitat ( $10^0$  m) to larger spatial scales like the reach scale ( $\sim 10^1 - 10^2$  m or  $20 \times$  the bankfull width, Fig. 1).

**Spot:** Measurements at sampling spots characterize biological and physical diversity at scales relevant to microbial communities (microscale). Depending on the cover of biofilm, this scale corresponds to at least an area of  $3.64 \text{ cm}^2$  (the sample volume of an acoustic Doppler velocimeter, section 5.2.1).

**Patch:** Patch-scale measurements characterize the macroinvertebrate communities and the physical conditions to which they are exposed. Each patch comprises four spots (Fig. 1). The total area of a patch corresponds to a four-replicated macroinvertebrate sample taken with a Surber sampler ( $0.25 \text{ m}^2$ , section 7). Patches should be distributed along the reach according to the relative dominance of mesohabitats.

**Mesohabitat:** An area of homogenous hydromorphological conditions (e.g., water depth, width, slope, surface flow type, grain size) that encompasses hydromorphological units such as pools, riffles, or glides. The number of patches within each mesohabitat is area-weighted.

**Reach:** A reach refers to the extent of the restoration measure and represents the largest spatial scale examined in RESTOLINK.

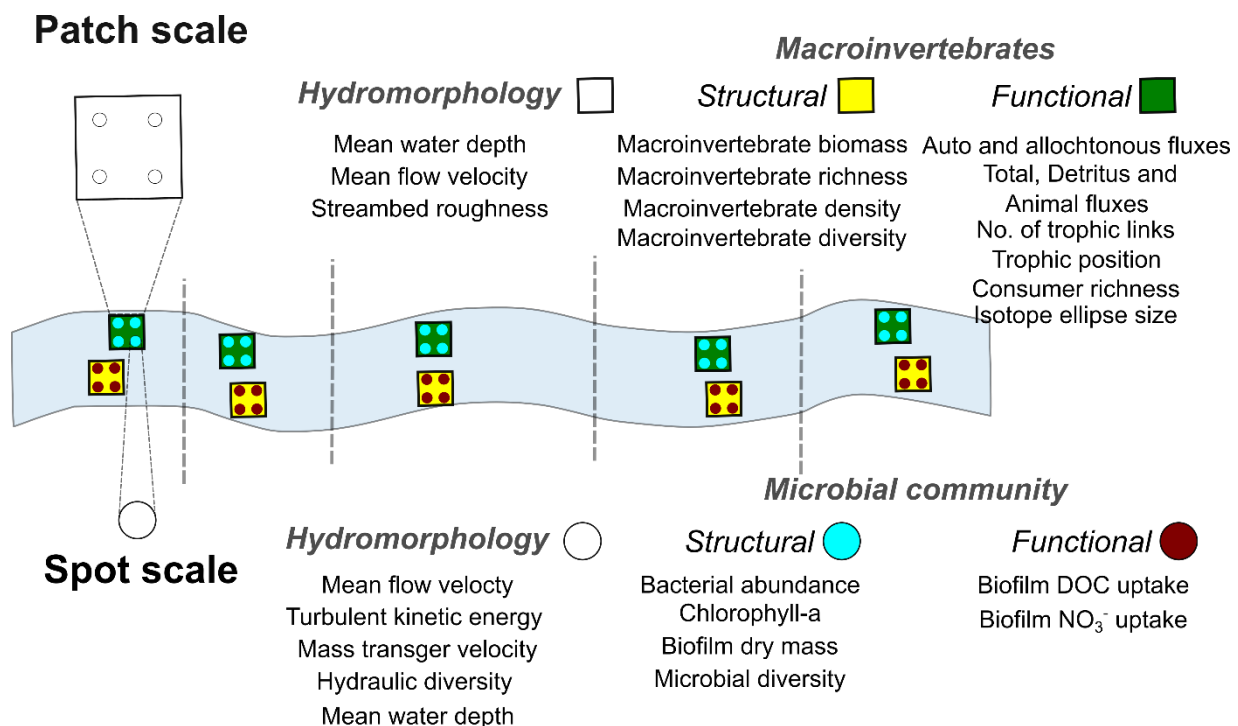


**Fig. 1.** Schematic overview of the nested sampling design. The number of sampling patches at which we conduct the measurements at patch scale and spot scale are defined by the number of mesohabitats present in each reach

#### 4. General sampling procedure

The overall sampling procedure is outlined below, for more details see sections 5 through 8. Note that for procedures specifically adapted to RESTOLINK, we include all necessary details, whereas for standard procedures, we refer to the original works. The general sampling procedure is as follows:

1. Define the start and end of each study reach.
2. Delineate mesohabitats and select sampling patches and spots:
  - i. Mesohabitats are visually determined according to the hydromorphological units present (pool, riffle, glide; section 3).
  - ii. According to the areal extent of each mesohabitat within the reach, distribute five pairs of patches (so that patches are distributed within the reach depending on the areal extent of each mesohabitat, i.e., area-weighted; Fig. 1). Mark the four corners of each patch with screws or flags (Fig. 2). The paired patches should be in proximity and exhibit comparable biological and physical conditions. From each pair of patches, we sample one before the stable isotope tracer addition and the other one at the plateau phase of the stable isotope tracer addition.
3. At the reach scale,
  - i. Delineate six water sampling stations (cross sections where water samples are taken): one upstream, one downstream of the reach and the other four spread equidistantly in between. Station one is the most upstream one.
  - ii. Expose loggers (e.g., light, temperature, stage, dissolved oxygen (DO)). We place two DO loggers at the first and last station for the two-station method for stream metabolism, or one DO logger at the last one for one-station approach is used (section 8.3).
  - iii. Perform propane addition and collect gas samples for greenhouse gas (GHG) fluxes (section 8.4).
4. Measure hydromorphological parameters at the reach, patch and spot scale (section 5; Table 2) except for grain size distribution that we perform at the end of the campaign (last point; section 5.2).
5. Sample biological parameters associated with the patches and spots sampled before the stable isotope tracer addition (sections 6 and 7; Table 2)
6. Conduct stable isotope tracer addition ( $^{15}\text{N}$ -nitrate and  $^{13}\text{C}$ -acetate, NaCl/NaBr) (section 8.1)
7. Sample biological parameters associated with stable isotope tracer addition (sections 6 and 7; Table 2)
8. Expose cotton strips and retrieve after 30 days (section 8.2).
9. After 7 days, retrieve DO sensors and loggers (section 8.3)
10. Perform pebble count measurements to determine reach-scale grain size (section 5.1).

**Table 2.** Overview of biological structural, functional, and hydromorphological parameters to be sampled at the three spatial scales.

Type	Spatial Scale	Parameter (units)
Structure	Spot	Bacterial abundance (cells m <sup>-2</sup> )
Structure	Spot	Chlorophyll- <i>a</i> (mg m <sup>-2</sup> )
Structure	Spot	Biofilm biomass (mg C m <sup>-2</sup> )
Structure	Spot	Microbial diversity
Function	Spot	Biofilm DOC uptake rate (mg DOC mg <sup>-1</sup> d <sup>-1</sup> )
Function	Spot	Biofilm N-NO <sub>3</sub> uptake rate (mg N-NO <sub>3</sub> m <sup>-2</sup> d <sup>-1</sup> )
Structure	Patch	Macroinvertebrate biomass (mg m <sup>-2</sup> )
Structure	Patch	Macroinvertebrate density (no. ind. m <sup>-2</sup> )
Structure	Patch	Macroinvertebrate richness (no. taxa)
Structure	Patch	Macroinvertebrate Shannon diversity (unitless)
Function	Patch	Autochthonous fluxes (J yr <sup>-1</sup> )
Function	Patch	Allochthonous fluxes (J yr <sup>-1</sup> )
Function	Patch	Animal fluxes (J yr <sup>-1</sup> )
Function	Patch	Detritus fluxes (J yr <sup>-1</sup> )
Function	Patch	No. Trophic links (number)
Function	Patch	Trophic position (unitless)
Function	Patch	Isotope ellipse size (‰ <sup>2</sup> )
Function	Patch	Consumer richness (no. taxa)
Function	Patch	Total fluxes (J yr <sup>-1</sup> )
Function	Reach	Organic matter decomposition (% d <sup>-1</sup> )
Function	Reach	Whole-reach DOC uptake rate (mg DOC m <sup>-2</sup> d <sup>-1</sup> )
Function	Reach	Whole-reach N-NO <sub>3</sub> uptake rate (mg N-NO <sub>3</sub> m <sup>-2</sup> d <sup>-1</sup> )
Function	Reach	Whole-reach Gross Primary Production (GPP; mg O <sub>2</sub> m <sup>-2</sup> d <sup>-1</sup> )
Function	Reach	Whole-reach Ecosystem Respiration (ER; mg O <sub>2</sub> m <sup>-2</sup> d <sup>-1</sup> )
Function	Reach	Whole-reach Net Ecosystem Production (NEP; mg O <sub>2</sub> m <sup>-2</sup> d <sup>-1</sup> )
Hydromorphology	Spot	Flow alpha diversity (unitless)
Hydromorphology	Spot	Mean flow velocity (m s <sup>-1</sup> )
Hydromorphology	Spot	Turbulent kinetic energy (m <sup>2</sup> s <sup>-2</sup> )
Hydromorphology	Spot	Mass transfer velocity (m s <sup>-1</sup> )
Hydromorphology	Spot	Mean water depth (m)
Hydromorphology	Patch	Flow alpha diversity (unitless)
Hydromorphology	Patch	Mean flow velocity (m s <sup>-1</sup> )
Hydromorphology	Patch	Streambed roughness
Hydromorphology	Reach	Mean water depth (m)
Hydromorphology	Reach	Mean stream width (m)
Hydromorphology	Reach	Reach bed slope
Hydromorphology	Reach	Mean flow velocity (m s <sup>-1</sup> )
Hydromorphology	Reach	Discharge (L s <sup>-1</sup> )
Hydromorphology	Reach	Canopy cover (%)
Hydromorphology	Reach	Grain size distribution (d <sub>10</sub> , d <sub>50</sub> and d <sub>84</sub> )

## 5. Hydromorphology

### 5.1 Spot- and patch-scale hydromorphology

For spot and patch-scale hydromorphology, we follow Anlager (2023, Appendix I).

#### 5.1.1 Hydraulic descriptors at the spot scale

We determine the hydraulic descriptors (Mean flow velocity, Turbulent kinetic energy, Mass transfer velocity, and Hydraulic diversity.) at the spot scale as close to the streambed as possible. Near-bed velocity fluctuations are important for microbial communities and macroinvertebrates (Biggs et al. 1998; Statzner et al. 1988). This measurement defines the spot-scale size within RESTOLINK, the sampling volume of an acoustic velocity meter, where the instrument averages velocity fluctuations.

#### Material list

- Holding frame for ADV (Fig. 2)
- ADV (Vectrino Profiler, Nortek AS, Norway; or other high-frequency devices))
- Computer
- Battery or generator to run the ADV and computer
- Waterproof photo camera
- Waterproof laser pointer
- Flags or metal nuts to mark measured points for later sampling (Fig. 2)
- Aquascope
- Ruler

#### Field instructions (for ADV)

1. Positioning of frame with attached ADV (e.g., at each sampling spot; watch out that tripod legs do not disturb flow in the vicinity of the ADV (Fig. 2))
2. Lowering ADV to 75mm between the transducer and the streambed. Under these conditions, the sweet spot of the instrument, for which velocity and turbulence measurements are most reliable, is located at 23 mm above the streambed (Brand et al. 2016; Koca et al. 2017)
3. Set expected measurement range for flow velocity and start data collection, check the histogram for phase wrapping (in particular, in fast-flowing areas), and adjust velocity range if necessary.
4. Start recording data for at least 10 min, which is sufficiently long for providing accurate characteristics of turbulence and facilitates spectral analysis of turbulent velocity fluctuations (Buffin-Bélanger & Roy, 2005). Sampling frequency 64 Hz.
5. For Vectrino Profiler: use maximal ping interval, except for very slow-flowing areas (e.g., impoundments: minimum ping interval, or increase sampling volume with max sampling volume)
6. Mark the sampling location (e.g., with a little screw downstream of the sampling area) and take a macro picture with a laser pointer to highlight the precise location of the flow measurement on the bed. We use the photograph to identify the sampling location for later biofilm sampling (Fig. 2).





**Fig. 2.** Left, holding frame for ADV (section 5.2.1) adapted from a tripod for a total station, with attached Vectrino Profiler (Nortek AS, Norway) measuring high-frequency flow velocity at 2 cm above the stream bed. Custom made for RESTOLINK. Right. Underwater photos of the sampling location are marked with a metal nut and a laser pointer indicating the precise sampling spot.

### Post-processing

Following Anlanger et al. (2021) and Anlanger (2023, Appendix I) we process the velocity time series. Briefly, we filter raw data with a threshold of 15 dB for the signal-to-noise ratio and 70% for signal correlation. We despoke the filtered velocities following Goring & Nikora (2002), modified by Wahl (2003). The nearest valid data points replace outliers, and the resulting velocity vectors are rotated for  $u$ ,  $v$ , and  $w$  ( $\text{m s}^{-1}$ ) to denote the longitudinal, transversal, and vertical components of the mean flow velocity vector, respectively. We remove measurement noise from the final velocities by low-pass filtering and estimate the cutoff frequency of the filter from the power spectra of each velocity time series and each velocity component. We identify noise in the spectra as the breakpoint in spectral slope, where the spectra flatten at high frequencies.

### Data analysis

For more details on the parameters, see Anlanger (2023, Appendix I).

**Mean flow velocity:** We estimate the Reynolds averaged longitudinal flow velocity ( $u$ ,  $\text{m s}^{-1}$ ) as the arithmetic mean of the post-processed velocity measurements. Please note that the mean values of  $v$  and  $w$  are zero after rotation.

**Turbulent kinetic energy:** We estimate turbulent kinetic energy ( $TKE$ ,  $\text{m}^2 \text{s}^{-2}$ ) from turbulent velocity fluctuations ( $u$ ,  $v$ ,  $w$ ;  $\text{m s}^{-1}$ ) by subtracting the mean values from measured (instantaneous) velocity components:  $TKE = 0.5 (\overline{u'^2} + \overline{v'^2} + \overline{w'^2})$ , the overbar denotes temporal averaging.

**Mass transfer velocity:** We estimate mass transfer velocity ( $k$ ,  $\text{m s}^{-1}$ ) according to Katul & Liu (2017):  $k = \alpha_1 (\epsilon \nu)^{0.25} Sc^{-0.5}$ , where  $Sc$  is the Schmidt number, which is the ratio of the kinematic viscosity of water ( $\nu$ ,  $\text{m}^2 \text{s}^{-1}$ ) depending on water temperature, and the molecular diffusion coefficient of the compound under study (i.e., nitrate and dissolved organic carbon).  $\alpha_1$  is a dimensionless scaling factor and was chosen to be 0.4 (Lorke et al. 2019). We obtain the dissipation rate of turbulent kinetic energy ( $\epsilon$ ,  $\text{W kg}^{-1}$ ) from fitting power spectra of vertical velocity fluctuations to theoretical spectra within the inertial subrange (inertial dissipation technique; Bluteau et al. 2011).

**Hydraulic diversity and extrapolation to larger scales:** We use a nested design to calculate  $\alpha$ , ( $\beta$ , and  $\gamma$  diversity of flow and morphology at different spatial scales. With this approach, we can account for the temporal and spatial variability of flow and morphology, and we can directly relate it to biological diversity measures (e.g.,  $\alpha$ ,  $\beta$  and  $\gamma$  diversities based on richness, Shannon diversity, Bray-Curtis similarity). See Anlager (2023, Appendix I) for further details.

### 5.1.2 Morphological measurements at the patch scale

We measure streambed roughness and water depth at this scale because they affect hydraulic habitat and mixing processes at the benthic interface (Lamarre & Roy, 2005; Noss & Lorke, 2016). We assess streambed topography using a custom-made laser scanner, following Noss & Lorke (2016) and Noss et al. (2018). We base the measurements of riverbed elevation on the principle of laser triangulation, resulting in a topographic map with x, y, and z coordinates (i.e., a digital elevation model, DEM). We illuminate the streambed with a laser line and observe it with two cameras (Fig. 3). We reconstruct the bottom elevation along the laser line from the location of the laser line. We mount the laser and cameras on a rack, which can move in a horizontal plane at an adjustable height above the bottom (Fig. 4). We track the horizontal position by a third camera out of water observing the position of an LED attached to the vertical rod.

#### Material list

- Costume made holding frame (Fig. 4)
- 3 GoPro cameras with waterproof housing
- Red line laser with waterproof housing (custom-made for RESTOLINK)
- LED light in splashproof housing
- Checkered board for calibration
- Ruler

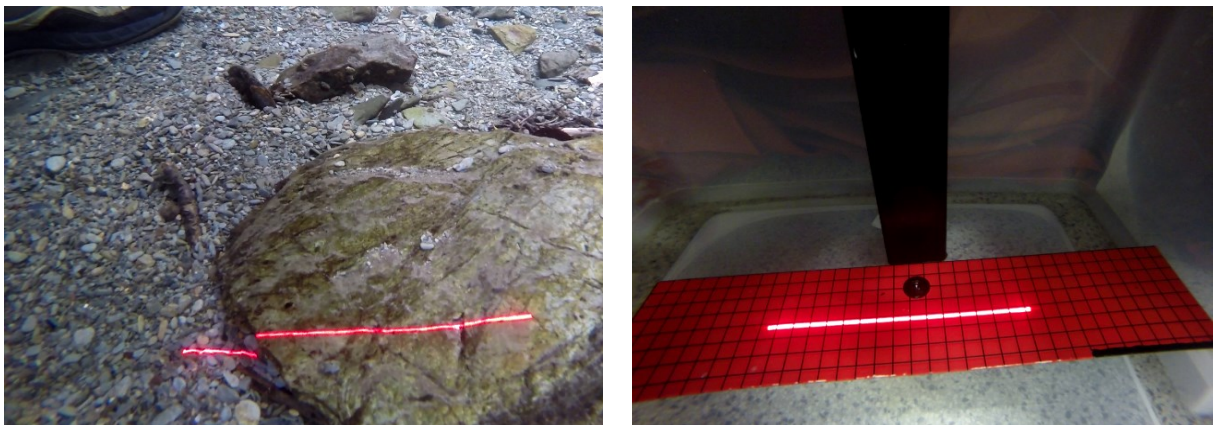


**Fig. 3.** Streambed topography is measured by a laser line, which is recorded by underwater cameras (left). The calibration procedure includes recording the laser line on a calibration board at different distances ranging from minimum to maximum water depths (right).

### Field instructions

1. Mounting of cameras, laser, and LED: Ensure that all camera angles and distances are adjusted for the local water depths while still maintaining the laser line on the streambed. The camera angle needs to be adjusted to always maintain a clear view of the LED.
2. Placing and leveling the rack above the patch
3. Start cameras, laser and LED and synchronize the cameras by a sudden movement that all cameras can see.
4. Adjust the vertical position of the laser and the two cameras so that they are submerged.
5. Carefully move the laser line along the horizontal direction of the frame. During laser deployment, cover the deployment frame with lightproof fabric to improve the visibility of the reflected laser line on the bed.
6. For each horizontal laser deployment, read the distance to the water surface from a marked reference point on the laser holding vertical unit.
7. Move the rack to a new measurement location and repeat the scanning until the whole patch is scanned. In case the cameras turn off during replacement, make sure to synchronize their internal clocks after restarting them.
8. For the conversion from pixel to metric coordinates, calibrate the laser line in a large bucket as outlined in Noss & Lorke (2016): observe the laser line on a calibration board at different distances from the laser ranging from minimum to maximum water depths (Fig. 2). Calibrate the position of the LED at varying distances, covering the whole horizontal movement

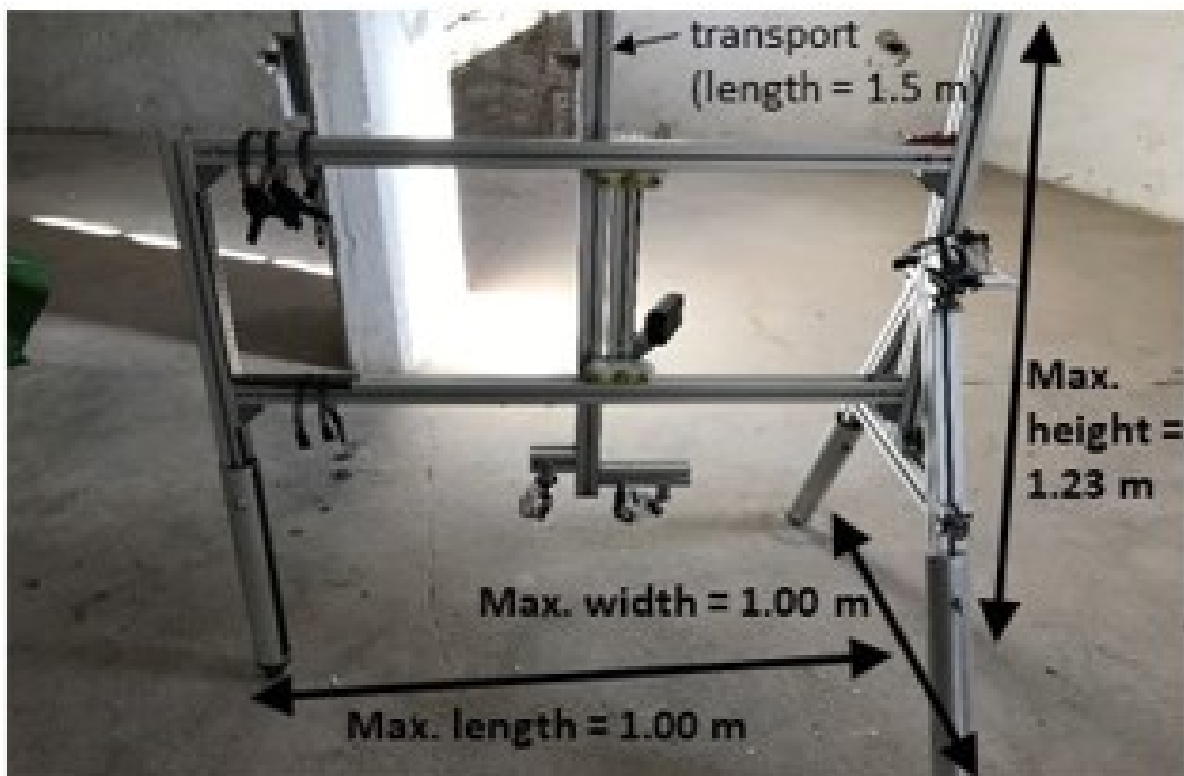


**Fig. 4.** Costume made, holding frame for morphological measurements at the patch scale.

## Post-processing

Before processing the recorded data, we synchronize videos from all three cameras by noting the time of the synchronization sign. We collect frames from the calibration procedure for each position recorded and later use them to translate each pixel into metric coordinates. Finally, we interpolate the DEM on a regular grid with a final horizontal resolution of 0.2 cm (i.e., medium sand) to reduce the data load while still representing the roughness of the most common grain sizes.

## Data analysis

***Streambed roughness and water depth:*** We estimate streambed roughness  $k$  as the standard deviation of the streambed elevation with respect to a planar surface, which is fitted to each DEM.

***Geomorphological diversity and extrapolation to larger scales:*** same procedure as for hydraulic diversity except for geomorphological  $\alpha$  diversity, which we calculate as the variance of water depth  $h$  normalized by the square of the mean depth at each patch.

## 5.2 *Reach-scale hydromorphology*

We determine reach-scale hydromorphological parameters, such as mean water depth, mean stream wetted width, water level and bed slope, mean flow velocity, and following Hauer and Lamberti (2017) (Table 2).

For reach-scale grain-size distribution ( $d_{10}$ ,  $d_{50}$  and  $d_{84}$ ), we use the Pebble count method (Polvi, Nilsson, & Hasselquist, 2014). Check out this video for more details <https://www.youtube.com/watch?v=mJMJ4O-qIDs>. From the cumulative sediment grain size distribution, we obtain  $d_{10}$ , the particle diameter representing the 10% cumulative percentile value;  $d_{10}$  is the effective diameter that controls porosity and hydraulic conductivity (Bear, 1988; Ren & Santamarina, 2017). The particle diameters representing the 50th and 84th percentile values,  $d_{50}$  and  $d_{84}$ , provides information on scouring and streambed instability (Bunte and Abt, 2001).

## 6. Microbial community structure and function (spot scale)

The determination of microbial community structure and function (spot-scale, Fig. 2) parameters comprises three steps: sampling, field processing, and laboratory processing (including data processing and/or calculations). Refer to Fig. 5 for an overview of the sampling and field processing procedures. Note that for Chlorophyll-a and bacterial abundance, we sample before the addition of the stable isotope tracer (section 8.1, Fig. 5), and for the other parameters of the microbial community during the stable isotope tracer addition (section 6.2.2, Fig. 5).

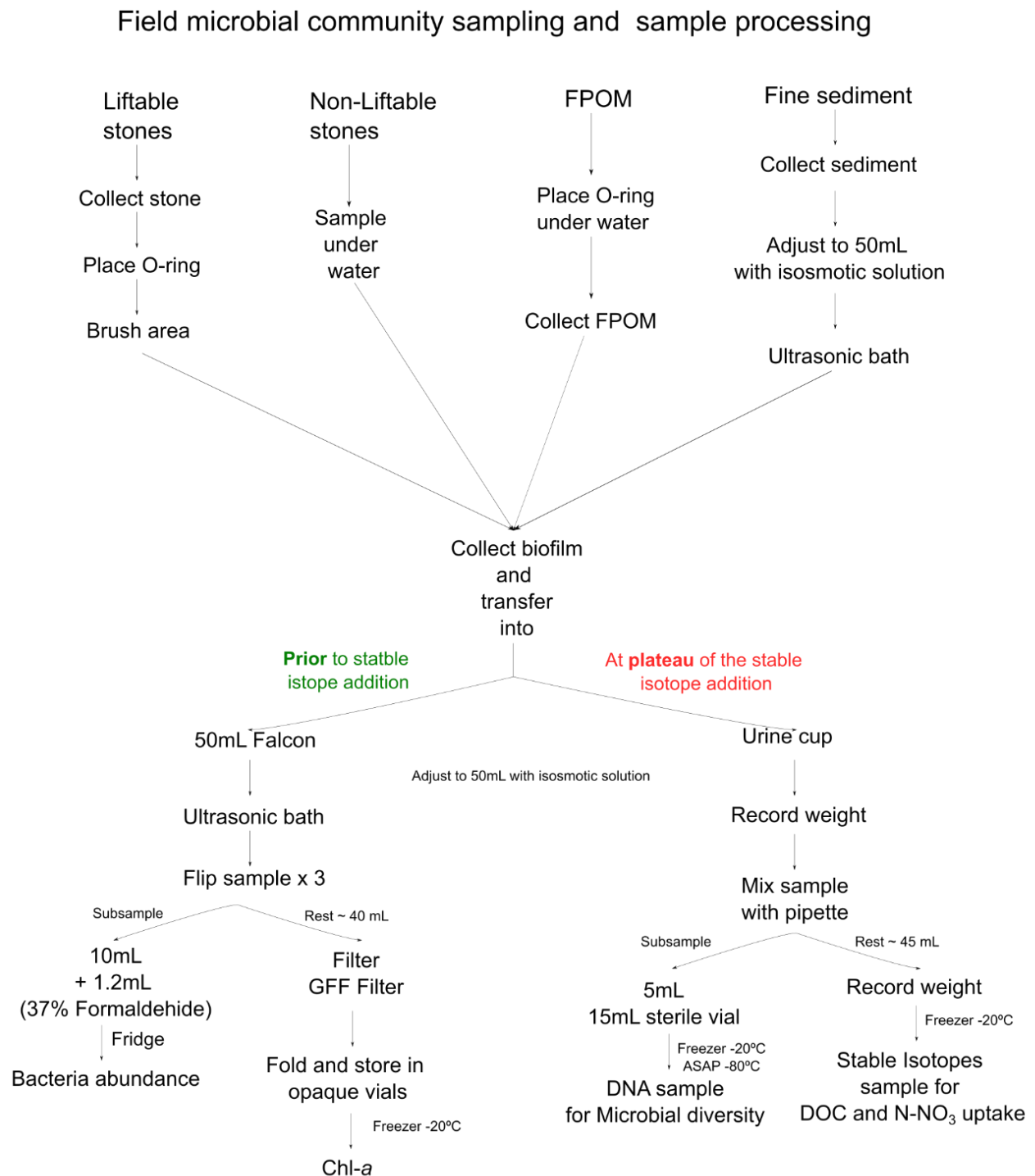


**Fig. 5.** Microbial sampling and field processing, for details, section 6.



## 6.1 Microbial community sampling

We have developed a substrate-specific microbial community sampling procedure. We identify four substrate types: cobbles, which can be lifted; boulders, which cannot be lifted; fine particulate organic matter (FPOM); and fine mineral substrate (coarse cobbles and finer).

Material list *Note that, depending on the substrate, material varies.*

- O-ring Ø 5cm (19.63 cm<sup>2</sup>)
- Tweezers
- Isosmotic solution (following DIN EN ISO 7346-3, doi: 10.31030/7468519)
- Toothbrush (one per sample)
- Funnel
- 50mL Falcon tubes
- Urine cups
- 60 mL syringes
- Biofilm sampler (Peters *et al.* 2005)

### Sampling for cobbles (liftable)

1. Gently lift the stone and place it in a tray without stream water.
2. Using the corresponding reference photo, place the O-ring on the target spot (section 5.1, Fig. 2).
3. If macroinvertebrates are present, use tweezers to remove them
4. Rewet the biofilm at the target spot using an isosmotic solution.
5. Brush the stone as demonstrated here:  
<https://www.youtube.com/watch?v=1aeHoh1RQpl> [at the 3.09-minute mark].
6. Transfer the biofilm slurry with a funnel into a 50 mL Falcon tube for bacteria abundance and Chlorophyll-a; otherwise into a urine cup and adjust to 50 mL with isosmotic solution (Fig. 5).

### Sampling boulders (not liftable)

1. Sampling is done underwater using a biofilm sampler (Peters *et al.* 2005).
2. Transfer the collected volume into a Falcon tube if the sample is for bacterial abundance and Chlorophyll a; otherwise into a urine cup adjusting to 50 mL with isosmotic solution.

### Sampling for sediment covered with FPOM

***Do not lift stones if they are covered by FPOM, as this will disrupt the microbial communities.***

1. Underwater, place the O-ring on the designated sampling spot.
2. Carefully collect the deposited FPOM with a 60mL syringe
3. Transfer the FPOM into a 50 mL Falcon tube, if the sample is for bacterial abundance and Chlorophyll-a, otherwise into a urine cup adjusting to 50 mL with isosmotic solution.

### Sampling for sediment smaller than coarse cobbles

1. Collect surface sediment from the top 1-2 cm using a small core (e.g., a 60-mL syringe with a cut tip or an inverted urine cup), assisted by a plastic plate.
2. Transfer the sediment sample into a 50-mL Falcon tube.
3. Adjust the volume to 50 mL by adding isosmotic water.
4. Sonicate the sample once for 3 minutes.
5. Transfer the supernatant into a 50-mL Falcon tube if the sample is for bacterial abundance and Chlorophyll-*a*, otherwise into a urine cup.
6. Adjust the volume to 50 mL by adding isosmotic or distilled water.

### 6.2 *Field processing of microbial samples*

As shown in Fig. 5, for field processing, we follow two different procedures depending on the targeted parameters: one for Bacterial abundance and Chlorophyll-*a*, and one for microbial diversity and Biofilm DOC and N-NO<sub>3</sub><sup>-</sup> uptake.

Material list *Note that, depending on the substrate, material varies.*

- Isosmotic solution (following DIN EN ISO 7646-3) or deionized water
- 50 mL and 15 mL sterile Falcon tube
- Ultrasonic bath
- 37% Formaldehyde
- Whatman GFF filter 47 mm
- Filtration column and pump (manual or electric)
- Gloves
- Trays
- Aluminum foil
- Scissors
- Pipette and tips
- Tweezers
- Opaque container for filter storage
- Scale
- Fridge/cooling box
- Freezer

#### 6.2.1 *Bacteria abundance and Chlorophyll-a*

1. After transferring the sample to the Falcon tube (last step from section 6.1), sonicate the sample for 2 minutes at 125 W and 400 kHz.
2. Gently flip the sample three times and transfer 10 mL into a 15 mL Falcon tube with 1.2 mL of 37% formaldehyde (4% v/v final concentration) for bacterial abundance. Store in the fridge.
3. Make a note of the remaining volume.
4. For Chlorophyll-*a*: Filter the remaining volume (≥40 mL) through Whatman GFF filter (Ø 47 mm). Place the filter on a tissue, fold it once and split it into two pieces using tweezers. Place the pieces into opaque vials and press them to the bottom. Freeze at -20°C.

### 6.2.2 *Microbial diversity and stable isotope uptake*

1. After transferring the sample to the urine cup (last step from section 6.1, Fig. 5), use a scale with precision to one decimal place of a microgram and record the weight of both the Urine cup and the sample.
2. Ensure thorough mixing of the sample aspirating and dispensing 5 mL back into the sample using a new pipette tip. Repeat three times.
3. With the same tip, withdraw 5 mL from the sample and place it into a 15 mL sterile Falcon tube for DNA extraction. Note: For DNA analysis, 0.5 mg dry mass is required, adapt volume if needed. Freeze at -80°C immediately or keep cool till the freezer is reached.
4. Weigh again the urine cup with the remaining volume sample, note it down and freeze immediately at -20°C or keep cool till then preserve for Biofilm  $^{13}\text{C}$ -DOC and  $^{15}\text{N}$ - $\text{NO}_3^-$  uptake (section 6.3.4)

## 6.3 *Microbial community laboratory analysis and data processing*

### 6.3.1 *Bacterial abundance*

For bacterial extraction and counting, we conduct flow cytometry following Perujo et al. (2017). For cases with low abundances, we use the DAPI counting method (Hobbie et al. 1977; Kamjunke et al. 2015).

### 6.3.2 *Chlorophyll-a*

Chlorophyll-a is photometrically analyzed in the biofilm suspension according to DIN 38412-16:1985-12.

### 6.3.3 *Microbial diversity*

We use standard extraction and amplification protocols using the DNeasy Blood & Tissue Kit or DNeasy Powersoil Pro Kit (Quiagen), or the NucleoSping Soil kit (MACHEREY-NAGEL GmbH & Co, KG) as described in (Groendahl et al. 2017).

### 6.3.4 *Biofilm $^{13}\text{C}$ -DOC and $^{15}\text{N}$ - $\text{NO}_3^-$ uptake*

After collecting the samples as outlined in section 6.2.2, we process them as follows to determine Biofilm  $^{13}\text{C}$ -DOC and  $^{15}\text{N}$ - $\text{NO}_3^-$  uptake and carbon (C) content as a proxy for biofilm biomass. For the processing and determination of the parameters, we adapted the method of Mulholland et al. (2004).

### Material list

- Freeze drier
- Tin foil capsules
- Precision scale (three decimals)
- Gloves
- 96-well microplate
- Tweezers
- Elemental analyzer



## Procedure

1. Once in the lab, freeze-dry or oven-dry the samples for at least 24 hours. Alternatively, samples can be filtered, dried, and the organic material can be scraped off the filter for analysis.
2. Transfer ~3 mg of biofilm sample and weigh into tin capsules using a precision scale (one decimal on the microgram).
3. Stable isotopic composition is analyzed on an elemental analyzer, directly connected via an open split system to an isotope ratio mass spectrometer.

## Calculation

We calculate  $N-NO_3^-$  uptake and DOC uptake from biofilm samples following Mulholland (2004) and LINX II protocol ([https://lter.kbs.msu.edu/docs/linx/linx2/linx2\\_protocols\\_15n\\_experiment.pdf](https://lter.kbs.msu.edu/docs/linx/linx2/linx2_protocols_15n_experiment.pdf)). We calculate biofilm uptake rates of  $^{13}C-DOC$  like for  $^{15}N-NO_3^-$ .

First, we convert the values into molar fraction (MF) and we calculated the  $^{15}N$  standing stock in biomass ( $mg\ ^{15}N\ m^{-2}$ ) as:

$$Tracer\ ^{15}N\ standing\ stock_{biomass} = DM * N\% * (MF_s - MF_b)$$

where DM is the biofilm dry mass ( $mg\ m^{-2}$ ), %N is the amount of N contained in the biofilm samples,  $MF_s$  is the molar fraction measured in the enriched biofilm sample while  $MF_b$  is the molar fraction measured and averaged from three biofilm samples collected upstream of the stable isotope tracer addition.

Then, we calculate the  $^{15}N$  fluxes in the stream water ( $Tracer\ ^{15}N\ flux_{water}$ ) and the total  $N-NO_3$  fluxes in the water ( $Total\ N - NO_3\ flux_{water}$ ) as:

$$Tracer\ ^{15}N\ flux_{water} = (MF_i * N - NO_3^- * Q) - (MF_b * N - NO_3^- * Q)$$
$$Total\ N - NO_3\ flux_{water} = [N - NO_3] * Q$$

where  $MF_i$  is the molar fraction measured in the water sample collected at plateau of the stable isotope tracer addition,  $MF_b$  is the molar fraction measured in the water samples collected upstream of the stable isotope tracer addition point, Q is the mean discharge measured at the water stations ( $L\ s^{-1}$ ),  $[N-NO_3]$  is the mean concentration measured in the water samples.

We then calculate biofilm  $^{15}N-NO_3^-$  uptake rate ( $mg\ ^{15}N-NO_3^-\ cm^{-2}\ d^{-1}$ ) as:

$$Biofilm\ ^{15}N - NO_3^- uptake = 2 \times \frac{Tracer\ ^{15}N\ standing\ stock_{biomass}}{\frac{Tracer\ ^{15}N\ flux\ water}{Total\ N - NO_3\ flux_{water}}}$$

We multiply uptake rates by 2 to express values per day as the stable isotope tracer addition lasts 12h.

## 7. Macroinvertebrates structure and function (patch scale)

We collect macroinvertebrate samples from patches previously defined by hydraulic measurements and marked with flags (section 5, Fig. 2). From each patch, we collect four replicated samples with a Surber sampler (500  $\mu\text{m}$  mesh, sampled area 0.25m<sup>2</sup>, Fig. 1) and pool them into a composite sample. We characterize the function and structure of the macroinvertebrate community from two pairing patches, one sampled for function before the addition of the stable isotope tracer (section 8), and another one for community structure at plateau following the addition of the stable isotope tracer.

### 7.1 Community structure

We preserve the samples in the field, sort them and count and identify individuals to the lowest taxonomic level feasible (usually genus level), except Diptera (family), Chironomidae (subfamily), Oligochaeta (order level), and Coleoptera larvae (family). From these data, we determine abundance, diversity and richness. From each taxon, we select at least 10 individuals to determine dry weight based on measurements of body dimensions and published length-mass relationships (See: dataset RESTOLINK – Macroinvertebrate Mass-Length relationships, [https:// 10.5281/zenodo.15984636](https://10.5281/zenodo.15984636)).

### 7.2 Function

We collect macroinvertebrate samples for stable isotope analysis from patches before the addition of the stable isotope tracer (section 8.1). We then sort and identify individuals to the lowest taxonomic level possible in the field under a stereomicroscope with up to 40 $\times$  magnification. We remove the guts from all omnivorous or predator species and analyze the gut contents under a microscope. We remove the shells of mollusks. If field processing is not feasible, we preserve the samples by freezing and subsequently process them in the lab.

Additionally, we sample putative organic matter resources, i.e., terrestrial particulate organic matter (t-POM), biofilm, benthic organic matter (BOM), and submerged macrophytes, alongside macroinvertebrate consumers. We collect samples for biofilm by brushing at least three stones per reach and filtering the resulting slurry through a 100  $\mu\text{m}$  mesh to remove coarse particles and immediately freezing it. We sample three replicates of streambed BOM using a sediment corer and sieve them through 100  $\mu\text{m}$ ; we freeze the fraction <100  $\mu\text{m}$  for later processing. We handpick terrestrial particulate organic matter, i.e., herbaceous vegetation and leaves from riparian trees, and submerged macrophytes (mostly moss), thoroughly rinse them, and freeze them for later processing.

Subsequently, we oven-dry macroinvertebrate consumers until they reach a constant weight and then freeze-dry them for 24 hours to extract putative organic matter resources. For stable isotope analysis, we ground samples of consumers and resources using an electronic ball mill and subsequently weigh them into tin capsules, which we analyze with an isotope ratio mass spectrometer (IRMS) linked to an elemental analyzer (EA).

We express stable isotope data as the relative difference between ratios of samples and standards (PeeDee Belemnite for  $\delta^{13}\text{C}$ , atmospheric  $\text{N}_2$  for  $\delta^{15}\text{N}$ ):

$$\delta R^{\text{‰}} = [(R_{\text{SAMPLE}}/R_{\text{STANDARD}}) - 1] \times 10^3$$

where  $R = {}^{13}\text{C}/{}^{12}\text{C}$  or  ${}^{15}\text{N}/{}^{14}\text{N}$ .

### 7.2.2 Trophic niche width

We calculate trophic niche width as the standard ellipse area corrected for small sample sizes (SEAc) using the SIBER R package (Jackson et al. 2011). We treat samples from patches as replicates for a given reach.

### 7.2.3 Food web - Mixing modeling

Prior to mixing model analysis, we identify outliers in the stable isotope data of consumers using simulated mixing polygons (Smith et al. 2013). The method generates 1,000 possible mixing polygons based on the mean and SD of resource stable isotopes using a Monte Carlo simulation and tests if consumers are located inside these polygons. For each consumer, we calculate the proportion of iterated polygons containing the respective consumer. We exclude consumers who are in less than 5% of the iterations (Smith et al. 2013). We account for trophic discrimination using factors and uncertainties specific to aquatic invertebrates:  $0.1 \pm 2.2\text{‰}$  for  $\delta^{13}\text{C}$  and  $2.6 \pm 2.0\text{‰}$  for  $\delta^{15}\text{N}$  (Brauns et al. 2018). We use Bayesian mixing models (simMR, Govan & Parnell, 2019), to estimate the contributions of biofilm, BOM, and t-POM to the diets of macroinvertebrate consumers found. We use the discrimination factors described above and model options with concentration dependence (Phillips & Koch, 2002) and without residual error terms (Parnell et al. 2013). We verify model convergence using the software's diagnostic plots and tests.

### 7.2.4 Organic matter fluxes

We use the “fluxweb” approach to estimate the energy flowing through the macroinvertebrate food web (Gauzens et al. 2019). The approach adopts a top-down perspective to calculate consumers’ energetic requirements from average body mass, abundance, allometric estimates of individual metabolic expenditures, and the fractional contribution of allo- and autochthonous resources to consumer diets. The latter uses either stable isotope mixing modeling (section 7.2.3) or functional feeding group information derived from the AQEM/STAR fuzzy coding categorization (Schmidt-Kloiber et al. 2006). From the resulting fluxes, we calculate i) allochthonous fluxes ( $\text{J m}^{-2}$ ) as the sum of fluxes flowing from terrestrial resources (leaves, herbaceous riparian vegetation) to macroinvertebrate consumers, ii) allochthonous fluxes as the sum of fluxes flowing from in-stream resources (biofilm, moss, submerged macrophytes), iii) detrital fluxes as the sum of fluxes from FPOM to macroinvertebrate consumers, and iv) animal fluxes as the sum of all predatory fluxes. To account for the uncertainty induced by i) within-reach variation in body mass and abundance, ii) variation of assimilation efficiencies, and iii) variation in metabolic rate exponents (Lang et al. 2017) required to calculate fluxes, we propagate uncertainties through the calculations. For each parameter, we generate a vector of 1,000 values drawn from a uniform distribution delimited by the upper and lower 95% percentile CI. We then calculate means and 95% bootstrapped confidence intervals of fluxes based on these values.

### 7.2.5 Food web structure

We assess food web complexity quantifying number of trophic links, consumers, and trophic levels based on consumer-resource matrices utilized for the calculation of organic matter fluxes and the “food web” package in R (Perdomo et al. under revision).

## 8. Ecosystem functioning (reach scale)

Ecosystem functioning at the reach scale comprises four main parameters (Table 2): whole-reach DOC and N-NO<sub>3</sub> uptake, organic matter decomposition, whole-reach metabolism and GHG fluxes.

### 8.1 Whole-reach DOC and N-NO<sub>3</sub> uptake

We measure whole-reach DOC and N-NO<sub>3</sub> uptake through Stable isotope tracer additions (<sup>13</sup>C, <sup>15</sup>N). The RESTOLINK stable isotope tracer addition expands on the procedure described in LINX II by including <sup>13</sup>C-DOC and <sup>15</sup>N-NO<sub>3</sub> uptake ([https://lter.kbs.msu.edu/docs/linx/linx2/linx2\\_protocols\\_15n\\_experiment.pdf](https://lter.kbs.msu.edu/docs/linx/linx2/linx2_protocols_15n_experiment.pdf); Mulholland et al. 2008). We enrich background bioavailable <sup>13</sup>C-DOC (10% of total DOC, 500‰ <sup>13</sup>C) and <sup>15</sup>N-NO<sub>3</sub> (2,000‰ <sup>15</sup>N) by a factor of 1.5x and 3x, respectively. We run 12h addition (6h night+6h daylight), after about 11h we sampled surface water following LINX II and microbial community (section 6 for details) and macroinvertebrate community (section 7.2 for details).

To determine the different reach-scale uptake metrics, we follow the standard procedures from Hall et al. (2009) and Abril et al. (2019). Briefly, we estimate the fractional N-NO<sub>3</sub> or DOC uptake rate per unit distance ( $k_w$ , m<sup>-1</sup>) from the regression of the ln-transformed tracer <sup>15</sup>N-NO<sub>3</sub> or <sup>13</sup>C-DOC flux versus distance downstream with data from the plateau samplings. We calculate the tracer <sup>15</sup>N-NO<sub>3</sub> or <sup>13</sup>C-DOC flux at each station by multiplying the background-corrected <sup>15</sup>N-NO<sub>3</sub> or <sup>13</sup>C-DOC concentration by discharge at each station. We calculate station-specific discharge from the dilution of the conservative tracer along the reach. The inverse of  $k_w$  is the uptake length ( $S_w$ ; m), which is converted to the mass-transfer velocity ( $V_f$ ; cm s<sup>-1</sup>) as the stream specific discharge ( $Q/w$ ) divided by  $S_w$ . We calculate the areal uptake rate ( $U$ ; µg m<sup>-2</sup> s<sup>-1</sup>), the mass of N-NO<sub>3</sub> or DOC taken up from the water column per unit streambed area and time, as  $V_f$  multiplied by the mean ambient NO<sub>3</sub> or DOC concentration. We calculate the areal assimilatory uptake rates by the entire microbial community (µg N m<sup>-2</sup> s<sup>-1</sup>).

### 8.2 Organic matter decomposition

We determine organic matter decomposition from cotton strips tensile-strength loss following the procedure developed by Tiegs et al. (2013). We place 10 cotton strips per reach, two strips per patch, and secure them to the stream bottom with metal rods. We incubate the cotton strips for 2-4 weeks in each reach.

### 8.3 Whole-reach metabolism (GPP, ER, NEP)

Gross primary production (GPP), ecosystem respiration (ER) and net ecosystem production (NEP = GPP – ER) integrate autotrophic and heterotrophic carbon fluxes over the benthic–pelagic interface. We estimate these fluxes from diel dissolved-oxygen (DO) dynamics, simultaneously solving for gas-exchange (reaeration) using Bayesian inverse models that incorporate an independent measurement with propane tracer as prior (Hall et al. 2016). DO loggers run for ≥72 h to capture more than two full diel cycles. When possible, we place the sondes in fully mixed mid-channel flow, avoiding back-eddies and emergent vegetation.

We use two complementary designs depending on reach scale hydraulics:

- Two-station, Lagrangian
  - Reach length  $0.4-1.0 \cdot v/K$  ( $v$  = mean velocity,  $K$  = night-time gas-exchange rate)
  - Two DO/temperature loggers: at upstream and downstream station
- One-station, Eulerian
  - Reach length  $> 3 \cdot v/K$  or hydraulically homogeneous over that distance
  - One DO/temperature logger at downstream station

Both designs share field instrumentation, gas exchange determination, and post-processing workflow; however, the model equation differs (section 8.3.2).

### 8.3.1 Gas exchange determination

We determine gas exchange using propane. Depending on logistics and reach characteristics, we determine gas exchange from a constant rate or a slug propane addition. Note that we do this together with the sampling for GHG fluxes (section 8.4).

Material list *Note that, depending on the method, material varies.*

- Gas diffuser
- Propane gas bottle
- Pre-evacuated 12mL exetainers
- 50mL syringes and needles

#### Constant-rate propane plateau

1. Diffuser set-up: Install a stainless-steel sparger (or silicone tubing with perforations) at  $\geq 25 \times$  wetted width upstream of station 1. Feed with a propane gas bottle.
2. Plateau target: Adjust flow to achieve fine bubbles. Maintain the addition for  $\geq 3$  nominal travel time to reach steady state along the reach.
3. Multi-station sampling: During plateau, collect triplicate (bubble-free) water samples at all six water-chemistry cross-sections plus one background site upstream of the diffuser (section 4). Extracting gas samples using the headspace method (section 8.4). Relative concentrations of propane gas are measured in the laboratory using GC-FID. Note down water temperature and sample temperature at headspace equilibration.

Deriving gas transfer velocity  $K$ : Fit an exponential decline of plateau concentration versus downstream distance:

$$\ln \frac{C_i}{C_0} = -\left(K \frac{z}{v}\right) x_i (\text{mean} \pm SD)$$

where  $x_i$  is downstream distance,  $z$  mean depth,  $v$  mean velocity. The resulting mean and SD form the prior for  $K_{600}$  in the Bayesian model.

Normalize the gas transfer velocity to  $K_{600}$ :

$$K_{600} = K \left( \frac{600}{Sc_{pp}} \right)^{-0.5}$$

where  $Sc_{pp}$  is the temperature-dependent Schmidt number for propane.

## Gas-exchange: slug propane addition

In the slug propane-addition method (Jin et al. 2012), a known volume of stream water enriched with dissolved propane and a conservative solute tracer is released instantaneously into the channel. As the tracer cloud travels downstream, water samples are collected at successive sites when the conductivity peak arrives, each sample being equilibrated with a known headspace and analyzed for propane concentration and the conservative solute. The concentration of propane is normalized by conservative solute concentration to correct for dilution. Then the natural logarithm of this ratio is plotted against the solute travel time (in hours) for each sampling site. The slope of the resulting linear regression,  $-K$ , yields the propane-specific gas-exchange rate  $K$  for that reach.

### 8.3.2 Bayesian inverse model

The two complementary designs (One- and two-station) are implemented following Hall et al. (2016). R scripts (1-station with  $K$  estimate. R, 2-station with  $K$  estimate. R; following) using Metropolis MCMC (mcmc package). They estimate four parameters: GPP, ER,  $K_{600}$ , and  $\log \sigma$  (residual SD). Chains run 100,000 iterations with proposal scale tuned to 20 % acceptance.

Parameter	Prior mean	Prior SD	Rationale
GPP ( $\text{g O}_2 \text{ m}^{-2} \text{ d}^{-1}$ )	Site-specific (ex. 0.3)	10% of mean (ex. 0.03)	Encourages rapid convergence while allowing $\pm 10\%$ variation.
ER ( $\text{g O}_2 \text{ m}^{-2} \text{ d}^{-1}$ )	Site-specific (ex. $-3.0$ )	10% of mean (ex. 0.3)	Should be broad enough to cover oligo- to mesotrophic reaches.
$K_{600}$ ( $\text{d}^{-1}$ ) $\log \sigma$	Propane mean $-2.3$	Propane SD 0.5	Tracer-informed. $\exp(-2.3) \approx 0.10 \text{ mg L}^{-1}$ — typical optical-sensor precision; SD allows $0.06$ – $0.17 \text{ mg L}^{-1}$ .

The parameters are obtained following these two equations for each of the designs:

- *Two-station (Lagrangian)*

$$O_{\text{down}}(t + \tau) = O_{\text{up}}(t) + \left( \frac{\text{GPP}}{z} \right) \left( \frac{I_{t \rightarrow t+\tau}}{I_{24h}} \right) + \left[ \frac{\text{ER}}{z} \right] \tau + K_{\tau} \Delta O_{\text{sat}}$$

where  $O_{\text{down}}(t+\tau)$  is the dissolved oxygen concentration in  $\text{mg O}_2 \text{ L}^{-1}$  at the downstream station at time  $t + \tau$ ;  $O_{\text{up}}(t)$  is the dissolved oxygen concentration in  $\text{mg O}_2 \text{ L}^{-1}$  at the upstream station at time  $t$ ;  $\tau$  is the travel time of a water parcel between stations, in d; GPP is gross primary production in  $\text{g O}_2 \text{ m}^{-2} \text{ d}^{-1}$ ; ER is ecosystem respiration in  $\text{g O}_2 \text{ m}^{-2} \text{ d}^{-1}$ ;  $z$  is the mean water depth in m;  $I_{t \rightarrow t+\tau}$  is the integrated photosynthetically active radiation in  $\mu\text{mol photons m}^{-2}$  received between  $t$  and  $t + \tau$ ;  $I_{24h}$  is the total daily integrated photosynthetically active radiation over 24 h;  $\Delta O_{\text{sat}}$  is the saturation deficit in  $\text{mg O}_2 \text{ L}^{-1}$ ;  $K_{\tau}$  is the reaeration contribution over  $\tau$  in  $\text{mg O}_2 \text{ L}^{-1}$ , calculated as  $K_{600} \times \tau \times (600/\text{Sc}(T))^{0.5}$ ;  $K_{600}$  is the gas-transfer velocity normalized to a Schmidt number of 600, in  $\text{d}^{-1}$ ;  $\text{Sc}(T)$  is the Schmidt number for  $\text{O}_2$  at water temperature  $T$  in Kelvin.

- *One-station (Eulerian)*

$$O(t) = O(t - \Delta t) + \left(\frac{GPP}{z}\right) \left(\frac{I(t)}{\sum I}\right) + \left[\frac{ER}{z}\right] \tau + K_{\Delta t} [O_{sat(t-\Delta t)} - O_{(t-\Delta t)}]$$

where  $O(t)$  is the dissolved oxygen concentration in  $\text{mg O}_2 \text{ L}^{-1}$  at time  $t$ ;  $O(t-\Delta t)$  is the concentration one logging interval earlier;  $\Delta t$  is the logging interval in days ( $5 \text{ min} \approx 0.003472 \text{ d}$ );  $GPP$  is gross primary production in  $\text{g O}_2 \text{ m}^{-2} \text{ d}^{-1}$ ;  $ER$  is ecosystem respiration in  $\text{g O}_2 \text{ m}^{-2} \text{ d}^{-1}$ ;  $\tau$  is the mean water in  $\text{m}$ ;  $I(t)$  is the instantaneous photosynthetically active radiation at time  $t$  in  $\mu\text{mol photons m}^{-2} \text{ s}^{-1}$ ;  $\sum I$  is the sum of instantaneous  $I(t)$  values over the full 24 h cycle for normalization;  $K_{\Delta t}$  is the reaeration contribution over  $\Delta t$  in  $\text{mg O}_2 \text{ L}^{-1}$ , given by  $K_{600} \times \Delta t \times (600/Sc(T))^{0.5}$ ;  $O_{sat}(t-\Delta t)$  is the  $\text{O}_2$  saturation concentration in  $\text{mg O}_2 \text{ L}^{-1}$  at temperature  $T$ , one interval earlier;  $K_{600}$  is the Schmidt-normalized gas-transfer velocity in  $\text{d}^{-1}$ ;  $Sc(T)$  is the Schmidt number for  $\text{O}_2$  at water temperature  $T$  in Kelvin.

### Convergence criteria

- Gelman–Rubin  $R\text{-hat} \leq 1.1$  for all parameters; otherwise rerun with broader priors or reduced proposal scale.
- Posterior unimodality confirmed by kernel density plots; bimodal fits are rerun similarly.

Posterior medians and 95 % credible intervals exported;  $NEP = GPP - |ER|$ .

### Reporting

- Metabolism:  $\text{g O}_2 \text{ m}^{-2} \text{ d}^{-1}$  (convert to  $\text{mg C}$  by  $\times 12/32$  if required).
- $K_{600}$ :  $\text{d}^{-1}$  and velocity  $k_{600} = K_{600} \cdot z$  ( $\text{m d}^{-1}$ ).
- Raw data, MCMC chains and auto-generated RMarkdown report archived.

### Assumptions and caveats

1. Linear light-production relationship: validated for gravel-bed biofilms; use Jassby–Platt option in script if saturation evident.
2. Constant  $ER$  over diel cycle: bias  $<10\%$  in summer; temperature-dependent  $ER$  module available if needed.
3. Well-mixed water column: avoid deep, stratified pools.

#### 8.4 Greenhouse gas (GHG) fluxes

We collect gas samples to assess GHG concentrations and fluxes at each of the six delimited stations along the study reach.

We use the headspace equilibration method to measure the partial pressures of CO<sub>2</sub> (pCO<sub>2</sub>), CH<sub>4</sub> (pCH<sub>4</sub>) and N<sub>2</sub>O (pN<sub>2</sub>O) in the three reaches. For this, we rinse syringes (60 mL) three times with stream water, fill them completely with stream water, empty them to leave 30 mL of stream water within the syringes, and add 30 mL of air by pointing the syringe upwards (far from our breath) and pulling the plunger slowly. After these steps, we close the stopcock, and the syringes have 30 mL of stream water and 30 mL of air. We shake them vigorously for 1 min and place them horizontally in the stream shoreline for 10 min for final water-air equilibration. We record the temperature during equilibration using a handheld sensor. Later, we insert a needle into the end of the stopcock at each syringe tip. Pointing upwards, we open the stopcock and immediately begin slowly pushing the plunger to expel the equilibrated air through the needle. When arriving at the 20 mL mark, we insert the needle through a septum into a pre-evacuated 12-mL exetainer (Labco, UK) and push the plunger to the end in order to transfer the 20 mL of equilibrated gas remaining in the syringe into the exetainer. For the air samples, we directly transfer 20 mL of ambient air to the exetainer, following the same aforementioned procedure (no equilibration or shaking is needed in this case). Then, we analyze the gas samples using a gas chromatograph (Goldenfum, 2011).

We determine aqueous CO<sub>2</sub>, CH<sub>4</sub> and N<sub>2</sub>O concentrations at field conditions headspace gas volume fractions and concentrations, based on the barometric pressure at the sampling site, field water temperature, laboratory equilibration temperature, and the appropriate Henry's law constants (Sander, 2015). Applying Fick's first law of gas diffusion, we determine fluxes across the water-air interface using the surface water and air partial pressures, the gas transfer velocities, and Henry's constants adjusted for temperature (Millero, 1995; Weiss, 1974). We determine the gas-specific transfer velocities for the three gases from K<sub>600</sub> estimated from propane additions (see above) using Schmidt-number scaling (Raymond et al. 2012).



## 9. References

- Abril, M., E. Bastias, D. von Schiller, E. Martí, M. Menéndez, Muñoz, I. (2019) Uptake and trophic transfer of nitrogen and carbon in a temperate forested headwater stream. *Aquatic Sciences* **81**: 75. doi: 10.1007/s00027-019-0672-x
- Anlanger, C., Risse-Buhl, U., von Schiller, D., Noss, C., Weitere, M., Lorke, A. (2021) Hydraulic and biological controls of biofilm nitrogen uptake in gravel-bed streams. *Limnology and Oceanography*, 66(11), 3887-3900. doi: 10.1002/lno.11927
- Anlanger, C. (2023) Interactions between flow hydrodynamics and biofilm attributes and functioning in stream ecosystems. RTPU. Doi: doi.org/10.26204/KLUEDO/7317
- Bear, J. (1988) *Dynamics of Fluids in Porous Media*, 2nd ed. American Elsevier Pub. Co.
- Biggs, B. J. F., Goring, D. G., Nikora, V. I. (1998) Subsidy and Stress Responses of Stream Periphyton to Gradients in Water Velocity as a Function of Community Growth Form. *Journal of Phycology*, 34(4), 598-607. doi: 10.1046/j.1529-8817.1998.340598.x
- Bluteau, C. E., Jones, N. L., Ivey, G. N. (2011) Estimating turbulent kinetic energy dissipation using the inertial subrange method in environmental flows. *Limnology and Oceanography: Methods*, 9(7), 302-321. doi: 10.4319/lom.2011.9.302
- Brand, A., Noss, C., Dinkel, C., Holzner, M. (2016) High-Resolution Measurements of Turbulent Flow Close to the Sediment–Water Interface Using a Bistatic Acoustic Profiler. *Journal of Atmospheric and Oceanic Technology*, 33(4), 769-788. doi: 10.1175/JTECH-D-15-0152.1
- Brauns, M., Boechat, I. G., de Carvalho, A., Graeber, D., Gücker, B., Mehner, T., von Schiller, D. (2018) Consumer-resource stoichiometry as a predictor of trophic discrimination ( $\Delta^{13}\text{C}$ ,  $\Delta^{15}\text{N}$ ) in aquatic invertebrates. *Freshwater Biology*, 63, 1240-1249. doi: 10.1111/fwb.13129
- Buffin-Bélanger, T., Roy, A. G. (2005) 1 min in the life of a river: selecting the optimal record length for the measurement of turbulence in fluvial boundary layers. *Geomorphology*, 68(1), 77-94. doi: 10.1016/j.geomorph.2004.09.032
- Bunte, K., Abt, S. R. (2001) Sampling Surface and Subsurface Particle-Size Distributions in Wadable Gravel- and Cobble-Bed Streams for Analyses in Sediment Transport, Hydraulics, and Streambed Monitoring, p. 428. In F. S. U.S. Department of Agriculture, Rocky Mountain Research Station [ed.]. Gen. Tech. Rep. RMRS-GTR-74. Fort Collins, CO.
- Gauzens, B., et al. (2019) fluxweb: An R package to easily estimate energy fluxes in food webs. *Methods in Ecology and Evolution*, 10(2), 270-279. doi: 10.1111/2041-210X.13109
- Goldenfum, J. A. (2011) GHG Measurement Guidelines for Freshwater Reservoirs. (UNESCO/IHA, 2011)
- Goring, D. G., Nikora, V. I. (2002) Despiking Acoustic Doppler Velocimeter Data. *Journal of Hydraulic Engineering*, 128(1), 117-126. doi:10.1061/(ASCE)0733-9429(2002)128:1(117)
- Govan E, Parnell A (2019). simmr: A Stable Isotope Mixing Model. R package version 0.5.1.216, <https://CRAN.R-project.org/package=simmr>.
- Groendahl, S., Kahlert, M., Fink, P. (2017) The best of both worlds: A combined approach for analyzing microalgal diversity via metabarcoding and morphology-based methods. *PLoS ONE* 12(2): e0172808. doi: 10.1371/journal.pone.0172808
- Hall, R., et al. (2009) Nitrate removal in stream ecosystems measured by  $^{15}\text{N}$  addition experiments: Total uptake. *Limnology and Oceanography* **54**: 653-665. doi: doi.org/10.4319/lo.2009.54.3.0653
- Hall, R.O., Tank, J.L., Baker, M.A., Rosi-Marshall, E.J., Hotchkiss, E.R. (2016) Metabolism, Gas Exchange, and Carbon Spiraling in Rivers. *Ecosystems*, **19**, 73-86. doi: 10.1007/s10021-015-9918-1
- Hauer & Lamberti (2017) *Methods in Stream Ecology*. Volume 1 Ecosystem structure, New York, Academic Press.
- Hobbie JE, Daley RJ, Jasper S (1977) Use of nuclepore filters for counting bacteria by fluorescence microscopy. *Applied and Environmental Microbiology*, **33**, 1225-1228. doi: 10.1128/aem.33.5.1225-1228.1977

- Jackson, A. L., Inger, R., Parnell, A. C., & Bearhop, S. (2011) Comparing isotopic niche widths among and within communities: SIBER - Stable Isotope Bayesian Ellipses in R. *Journal of Animal Ecology*, 80(3), 595-602. doi:10.1111/j.1365-2656.2011.01806.x
- Jin, H.-S., White, D. S., Ramsey, J. B., Kipphut, G. W. (2012) Mixed Tracer Injection Method to Measure Reaeration Coefficients in Small Streams. *Water, Air, & Soil Pollution*, 223, 5297-5306. doi: 10.1007/s11270-012-1280-8
- Kamjunke N, Herzsprung P, Neu TR (2015) Quality of dissolved organic matter affects planktonic but not biofilm bacterial production in streams. *Science of the Total Environment*, **506,Äi507**, 353-360. doi: 10.1016/j.scitotenv.2014.11.043
- Katul, G., Liu, H. (2017) Multiple mechanisms generate a universal scaling with dissipation for the air-water gas transfer velocity. *Geophysical Research Letters*, 44(4), 1892-1898. doi: 10.1002/2016GL072256
- Koca, K., Noss, C., Anlanger, C., Brand, A., Lorke, A. (2017) Performance of the Vectrino Profiler at the sediment–water interface. *Journal of Hydraulic Research*, 55(4), 573-581. doi: 10.1080/00221686.2016.1275049
- Lamarre, H., Roy, A. G. (2005) Reach scale variability of turbulent flow characteristics in a gravel-bed river. *Geomorphology*, 68(1), 95-113. doi: 10.1016/j.geomorph.2004.09.033
- Lang, B., Ehnes, R. B., Brose, U., Rall, B. C. (2017) Temperature and consumer type dependencies of energy flows in natural communities. *Oikos*, 126(12), 1717-1725. doi: 10.1111/oik.04419
- Lorke, A., Bodmer, P., Koca, K., Noss, C. (2019) Hydrodynamic control of gas-exchange velocity in small streams. *EarthArXiv*, 1-23. doi: 10.31223/osf.io/8u6vc
- Millero, F. J. (2005). *Chemical oceanography* (Vol. 30). CRC press.
- Mulholland, P. J. et al. (2004) Stream denitrification and total nitrate uptake rates measured using a field <sup>15</sup>N tracer addition approach. *Limnology and Oceanography* **49**: 809-820. doi: 10.4319/lo.2004.49.3.0809
- Mulholland, P. J., et al. (2008) Stream denitrification across biomes and its response to anthropogenic nitrate loading. *Nature* 452: 202-206. doi: 10.1038/nature06686
- Noss, C., Lorke, A. (2016) Roughness, resistance, and dispersion: Relationships in small streams. *Water Resources Research*, 52(4), 2802-2821. doi: 10.1002/2015WR017449
- Noss, C., Wilkinson, J., Lorke, A. (2018) Triangulation hand-held laser-scanning (TriHaLaS) for micro- and meso-habitat surveys in streams. *Earth Surface Processes and Landforms*, 43(6), 1241-1251. doi: 10.1002/esp.4310
- Parnell, A. Govan, E. (2019) simmr: A Stable Isotope Mixing Model. <https://CRAN.R-project.org/package=simmr>. .
- Parnell, A. C., et al. (2013) Bayesian stable isotope mixing models. *Environmetrics*, 24(6), 387-399. doi:10.1002/env.2221
- Perdomo, G., Sunnucks P., Thompson, R.M. (submitted) “food web”: an open-source program for the visualisation and analysis of compilations of complex food webs. Under revision in *Environmental Modelling and Software*.
- Perujo, N., Sanchez-Vila, X., Proia, L., Romaní, A. M. (2017) Interaction between Physical Heterogeneity and Microbial Processes in Subsurface Sediments: A Laboratory-Scale Column Experiment. *Environmental Science & Technology*, 51(11), 6110-6119. doi: 10.1021/acs.est.6b06506
- Peters, L., Scheifhacken, N., Kahlert, M., Rothhaupt, K. O. (2005) An efficient in situ method for sampling periphyton in lakes and streams. *Archiv für Hydrobiologie*, 163, 133–141. doi: 10.1127/0003-9136/2005/0163-0133
- Phillips, D. L., Koch, P. L. (2002) Incorporating concentration dependence in stable isotope mixing models. *Oecologia*, 130(1), 114-125. doi: 10.1007/s004420100786
- Polvi, L. E., Nilsson, C., Hasselquist, E. M. (2014) Potential and actual geomorphic complexity of restored headwater streams in northern Sweden. *Geomorphology*, 210, 98-118. doi: 10.1016/j.geomorph.2013.12.025

- Raymond, P. A., et al. (2012) Scaling the gas transfer velocity and hydraulic geometry in streams and small rivers. *Limnology and Oceanography: Fluids and Environments*, 2(1), 41-53. doi: 10.1215/21573689-1597669
- Ren, X., Santamarina, J.C. (2017) The hydraulic conductivity of sediments: A pore size perspective. *Engineering Geology* **233**: 48-54. doi: 10.1016/j.enggeo.2017.11.022
- Sander, R. (2015) Compilation of Henry's law constants (version 4.0) for water as solvent. *Atmos. Chem. Phys.* **15**, 4399–4981. doi: 10.5194/acp-15-4399-2015.
- Schmidt-Kloiber, A., Graf, W., Lorenz, A., Moog, O. (2006) The AQEM/STAR taxalist - a pan-European macroinvertebrate ecological database and taxa inventory. *Hydrobiologia*, 566, 325-342. doi: 10.1007/s10750-006-0086-3]
- Smith, J. A., Mazumder, D., Suthers, I. M., & Taylor, M. D. (2013) To fit or not to fit: evaluating stable isotope mixing models using simulated mixing polygons. *Methods in Ecology and Evolution*, 4(7), 612-618. doi:10.1111/2041-210X.12048
- Statzner, B., Gore, J. A., & Resh, V. H. (1988) Hydraulic stream ecology: observed patterns and potential applications. *Journal of the North American Benthological Society*, 7(4), 307-360. doi: 10.2307/1467296
- Tiegs, S.D., Clapcott, J.E., Griffiths, N.A., Boulton, A.J. (2013) A standardized cotton-strip assay for measuring organic-matter decomposition in streams. *Ecological Indicators*, **32**, 131-139. doi: 10.1016/j.ecolind.2013.03.013
- Wahl, T. L. (2003) Discussion of "Despiking Acoustic Doppler Velocimeter Data" by Derek G. Goring and Vladimir I. Nikora. *Journal of Hydraulic Engineering*, 129(6), 484-487. doi: 10.1061/(ASCE)0733-9429(2003)129:6(484)
- Weiss, R. F. (1974) Carbon dioxide in water and seawater: the solubility of a non-ideal gas. *Marine Chemistry* **2**: 203-215. doi: 10.1016/0304-4203(74)90015-2